SC42010 Robust and Multivariable Control

Design Project

7 April 2019

TU Delft
Coordinated by Prof Simone Baldi and Prof Giulia Giordano

Alexander Berndt 4698959 A.E.Berndt@student.tudelft.nl

Matthijs Bekendam 4725751 J.M.Bekendam@student.tudelft.nl

Contents

Introduction

This assignment considers the analysis and design of controllers for multiple input/multiple output (MIMO) systems as well as uncertainties. This is considerably more complicated than designing controllers for single input/single output (SISO) systems since the inputs and outputs of MIMO systems are often interconnected, meaning that we cannot simply design a controller from each input to each output respectively and guarantee the overall system to satisfy the performance specifications or even be stable for that matter.

Sophisticated analysis and controller synthesis tools have been developed which allow for the design of a controller which will (when possible) ensure stability and performance of MIMO systems. Additionally, by considering uncertainties in the system, these controllers can also be designed to ensure robust system stability and performance. These methods are further discussed in [2] and are explored throughout this assignment.

Robust Control for Missile Autopilot

In this assignment, we consider a MIMO system which denotes the dynamics of a missile autopilot system. This system is described in more detail in [1] but is summarized below for reference in this assignment.

$$
\begin{gathered}
\begin{bmatrix} \dot{\alpha} \\ \dot{q} \end{bmatrix} = \begin{bmatrix} -0.89 & 1 \\ -142.6 & 0 \end{bmatrix} \begin{bmatrix} \alpha \\ q \end{bmatrix} + \begin{bmatrix} 0 & -0.119 \\ 178.25 & -130.8 \end{bmatrix} \begin{bmatrix} w_\Delta \\ \delta \end{bmatrix} \\
\begin{bmatrix} \eta \\ q \\ z_\Delta \end{bmatrix} = \begin{bmatrix} -1.52 & 0 \\ 0 & 1 \\ -1 & 0 \end{bmatrix} \begin{bmatrix} \alpha \\ q \end{bmatrix} + \begin{bmatrix} 0 & -0.203 \\ 0 & 0 \\ 0 & 0 \end{bmatrix} \begin{bmatrix} w_\Delta \\ \delta \end{bmatrix} \\
w_\Delta = \Delta z_\Delta, \quad \Delta \in [-1, 1]
\end{gathered} \tag{0.1}
$$

The system states, inputs and outputs are as follows

States

- Angle of attack α
- Pitch rate q

Inputs

- Fin angle δ

Outputs:

- Measured acceleration in z-direction η
- Measured pitch rate q

Uncertainty:

- $\Delta \in [-1, 1]$

The system also has the auxiliary input w_Δ and output z_Δ used to model the effect of variations in the system dynamics. These model variations consider the different aerodynamic coefficients which are determined by angles of α between 0^o and 20^o.

1 Nominal Analysis and Controller Design

SISO Controller Design

Question 1

Using a SISO feedback loop (illustrated in Figure 1) we aim to control the acceleration η by only using η_c as reference input. This can be done without changing the structure of the original model by addition of the mapping matrices G_{in},G_{out} and R_{in}.

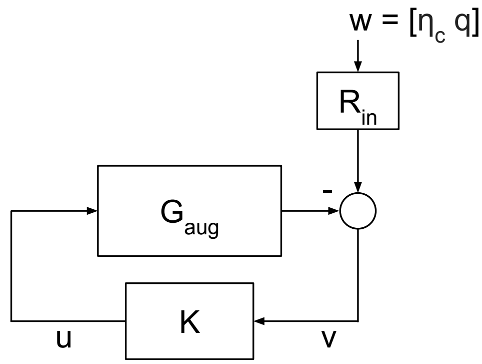

Figure 1: Augmented System G

The state space model of the augmented system G is derived from the original MIMO state space system as presented in [1] and the Introduction. The state space system represented by G_{aug} is as follows:

$$\begin{bmatrix} \dot{\alpha} \\ \dot{q} \end{bmatrix} = \begin{bmatrix} -0.89 & 1 \\ -142.6 & 0 \end{bmatrix} \begin{bmatrix} \alpha \\ q \end{bmatrix} + \begin{bmatrix} -0.119 \\ -130.8 \end{bmatrix} \delta$$

$$\begin{bmatrix} \eta \\ q \\ z_\Delta \end{bmatrix} = \begin{bmatrix} -1.52 & 0 \\ 0 & 1 \\ -1 & 0 \end{bmatrix} \begin{bmatrix} \alpha \\ q \end{bmatrix} + \begin{bmatrix} -0.203 \\ 0 \\ 0 \end{bmatrix} \delta$$

Question 2

In order to design a SISO controller for the nominal system, we follow the familiar loop-shaping approach. First, the frequency response of the open-loop transfer function $G_{11}(s)$ is plotted. This is represented by the blue line in Figure 2.

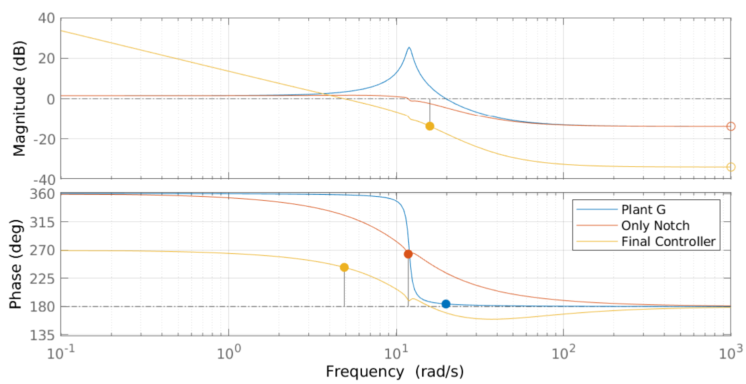

Figure 2: Bode Plot of Loop Shaping Design

We note a sharp peak at approximately 12.2 rad/s. Hence, we opt for a notch filter to remove this peak. We find a notch which centers at this peak by choosing $g_{min} = 0.05$, $\zeta = 0.7$, $\omega = 12.2$ rad/s as described in Equation 1.1.

$$N(s) = \frac{s^2 + 2g_{min}\zeta\omega s + \omega^2}{s^2 + 2\zeta\omega s + \omega^2} \tag{1.1}$$

The red line in Figure 2 represents G_{11} controlled with the notch in Equation 1.1. Since the magnitude plot is flat at low frequencies, we will not achieve zero steady state tracking error. To account for this, we consider a PI control form as shown in Equation 1.2 with $K_P = 0.1$, $K_I = 4$.

$$K_{PI}(s) = K_P + K_I \tfrac{1}{s} \tag{1.2}$$

The final controller uses the notch filter and the PI-controller in series. The open-loop bode plot is represented by the yellow line in Figure 2. The final controller is defined in Equation 1.3

$$K(s) = \left(0.1 + \tfrac{4}{s}\right) \frac{s^2 + 0.84s + 144}{s^2 + 16.8s + 144} \tag{1.3}$$

Question 3

The bode plot for the controlled open-loop system represented by the yellow line in Figure 2 is repeated in Figure 3. Additionally, the corresponding Nyquist plot is shown in Figure 4.

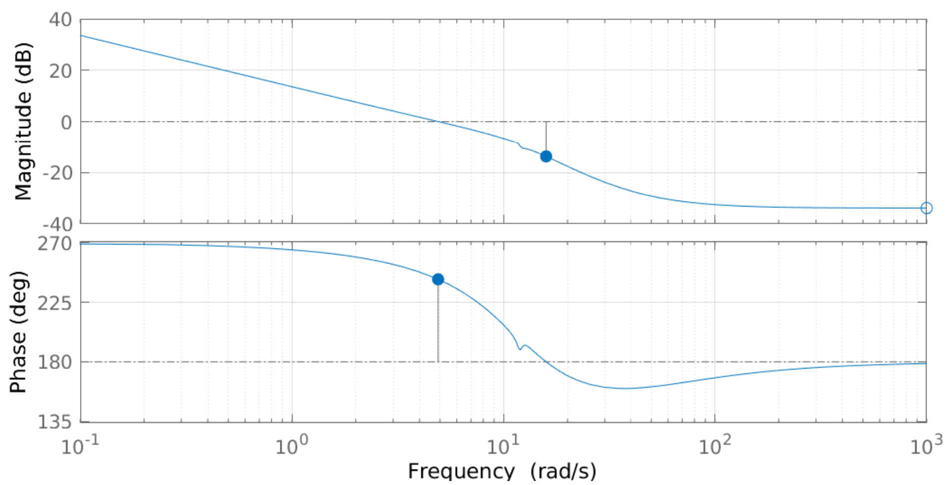

Figure 3: Bode Plot of Controlled Plant (PM = 62.4^o, GM = 13.7 dB)

From Figure 3, we note a bandwidth of 4.9 rad/s (0.78 Hz) with 62.4 degrees of Phase Margin and a Gain Margin of 13.7 dB. Positive gain- and phase margin indicate a stable closed-loop system for the full model from the input η_c to the output η. The stable gain- and phase margin values are also shown in the Nyquist plot of Figure 4. Since the Nyquist plot does not encircle the -1 point, we can conclude a stable closed-loop response since the plant has no RHP's. The large gap between the -1 point and the Nyquist plot for all frequencies also indicate good closed-loop system performance. This is confirmed in Question 4 in Figure 5.

Question 4

Using the Robust Toolbox of MATLAB, we plot the output variables for a step input η_c. The response is shown in Figure 5. Clearly the design conforms to the design specifications of zero steady-state error, minimal overshoot and bandwidth larger than 0.3 Hz.

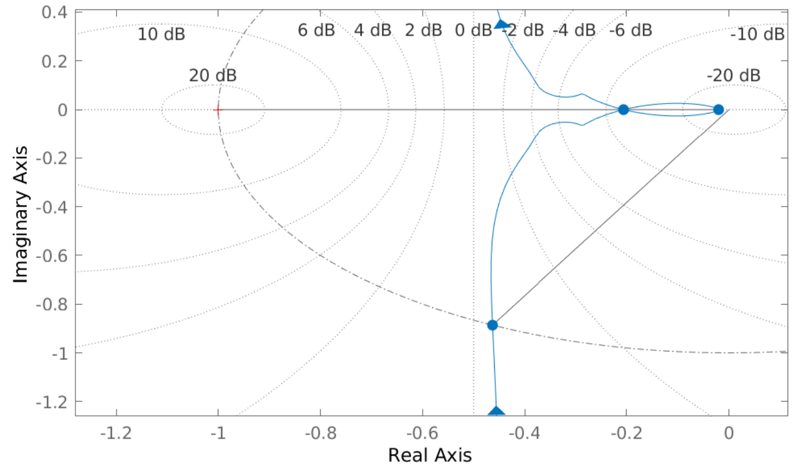

Figure 4: Nyquist Plot of Controlled Plant

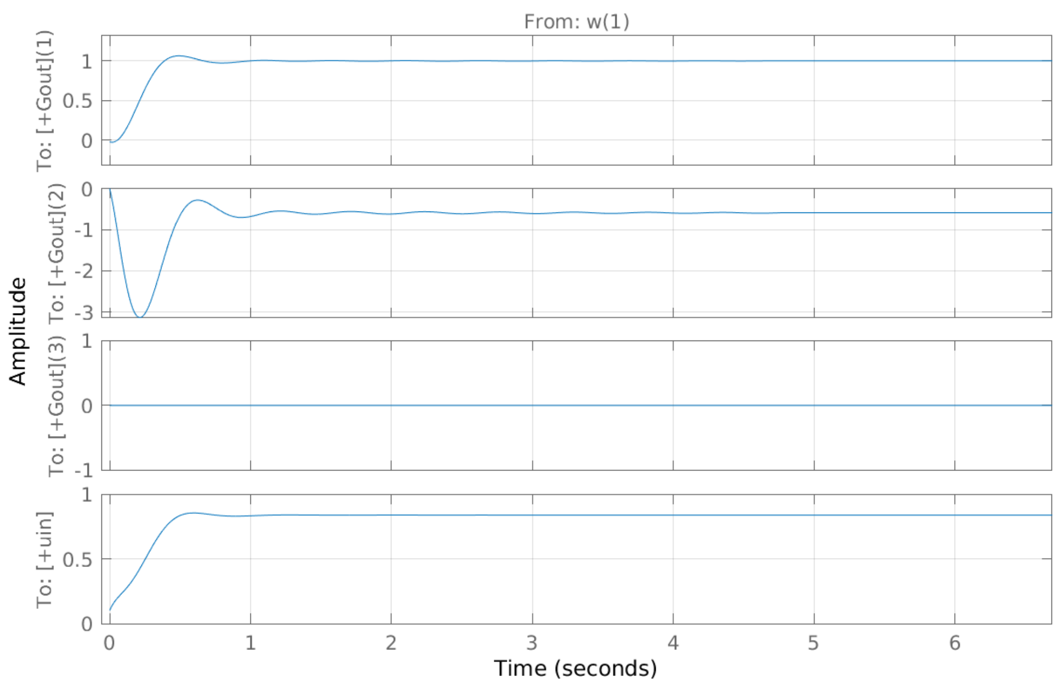

Figure 5: Step Response: η, q, z_Δ, δ (top-to-bottom)

The final performance parameters for the SISO $\eta_c - \eta$ tracking are

- Overshoot: 6.4%
- Settling time: 0.87s
- Rise time: 0.24s

MIMO Controller Design

Question 5

Using the whole system G, the following RGA matrices were found using the target bandwidths $\omega = 0$ and $\omega = 0.3 \cdot 2\pi$.

$$RGA_{\omega=0} = \begin{bmatrix} -4.36 & 5.11 \\ -1.50 & 1.76 \\ 6.87 & -5.87 \end{bmatrix}$$

$$RGA_{\omega=0.3\cdot 2\pi} = \begin{bmatrix} -5.59 + 2.14i & 6.52 - 2.14i \\ 4.65 - 3.17i & -3.85 + 3.17i \\ 1.94 + 1.03i & -1.67 - 1.03i \end{bmatrix}$$

Inspecting the RGA elements around the crossover frequency reveals that the system is not sensitive to input uncertainties, since all elements are relatively small. The RGA matrix at zero and the desired bandwidth also has small elements ($G_{ij} < 10$), meaning the system is not ill-conditioned and should not be too challenging to control. This conclusion is derived from the discussion in Section 3.4.5 in [2].

Question 6

G(s) has a pole at ω if some entry of G(s) has a pole at ω. The following MIMO poles were computed:

$$\text{MIMO Poles} = -0.445 \pm 11.93i$$

For MIMO system the zeros (z_i) are the inputs for which $G(z_i)$ loses rank. Since there are no values of z for which this happens in our system, there are no zeros.

It can be concluded that with the absence of any transmission zeros, there is no zero output for some non-zero input. Also since the complex pole pair is located inside the LHP, the system is stable

Question 7

The block diagram of the nominal MIMO system is shown in Figure 6. Note that we do not consider any uncertainty Δ since we are only analyzing the nominal system at this point. Since $\Delta = 0$, we can define the series interconnection of the plant G with it's associated mapping matrices as $G_{aug} = G_{out} G G_{in}$. We can equivalently define G_{aug} by only considering certain inputs and outputs as defined by G_{in} and G_{out} mapping matrices. Equation 1.4 explicitly defines the system mapped by G_{aug} where the input u of Figure 6 is the input δ in Equation 1.4.

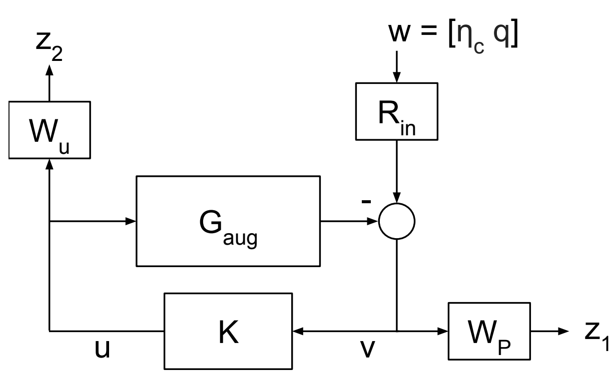

Figure 6: Block Diagram of Weighted Nominal MIMO System

$$
\begin{bmatrix} \dot{\alpha} \\ \dot{q} \end{bmatrix} = \begin{bmatrix} -0.89 & 1 \\ -142.6 & 0 \end{bmatrix} \begin{bmatrix} \alpha \\ q \end{bmatrix} + \begin{bmatrix} -0.119 \\ -130.8 \end{bmatrix} \delta
$$
$$
\begin{bmatrix} \eta \\ q \\ z_\Delta \end{bmatrix} = \begin{bmatrix} -1.52 & 0 \\ 0 & 1 \\ -1 & 0 \end{bmatrix} \begin{bmatrix} \alpha \\ q \end{bmatrix} + \begin{bmatrix} -0.203 \\ 0 \\ 0 \end{bmatrix} \delta \tag{1.4}
$$

The weighting matrices W_u and W_P are used to shape the input sensitivity KS and sensitivity functions S respectively. As defined in the assignment and [1], we use the weighting functions as defined in Equations 1.5 and 1.6.

$$
W_P = \begin{bmatrix} \frac{0.25s+0.6\pi}{s+0.0006\pi} & 0 & 0 \\ 0 & 0.08 & 0 \end{bmatrix} \tag{1.5}
$$
$$
W_u = \frac{0.001s^3 + 0.03s^2 + 0.3s + 1}{1e - 5s^3 + 3e - 2s^2 + 30s + 10000} \tag{1.6}
$$

Question 8

As discussed in Section 3.8.2 of [2], shaping S and KS is important because these functions fundamentally describe the stability, performance, robustness (and other properties) of the closed-loop system. Specifically, consider the following:

S **Sensitivity Function**
Shaping this function allows us to focus on the performance of the system since the sensitivity function essentially represents the bode plot of the tracking error. In the time-domain, performance refers to a fast rise time with small settling time. With a large $W_p(j\omega)$ at frequency ω, we penalize large tracking errors at this frequency. Similarly, a small $W_p(j\omega)$ at frequency ω allows for larger tracking errors around this frequency.

KS **Input Sensitivity Function**
Shaping this function allows us to determine the size of the allowable input at various frequencies. With a large $W_u(j\omega)$ at frequency ω, we penalize control inputs at this frequency. Similarly, a small $W_u(j\omega)$ will allow larger control inputs at this frequency.

T **Complimentary Sensitivity Function**
(Despite us not using a weighted T as an output, this is added for completeness)
Shaping this function gives us the ability to influence the robustness of the closed-loop system as well as it's sensitivity to noise.

Question 9

Assuming the need for controller synthesis, the generalized plant can be derived from the block diagram in Figure 6. This plant is defined by a system interconnecting P and K as shown in Figure 7. We do not add Δ since we only consider the nominal system in this case.

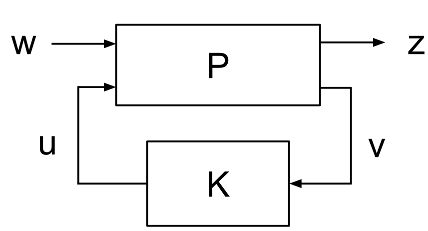

Figure 7: Interconnection of P and K

$$\begin{bmatrix} z \\ v \end{bmatrix} = \begin{bmatrix} P_{11} & P_{12} \\ P_{21} & P_{22} \end{bmatrix} \begin{bmatrix} w \\ u \end{bmatrix} \tag{1.7}$$

$$\begin{bmatrix} \begin{bmatrix} z_1 \\ z_2 \end{bmatrix} \\ v \end{bmatrix} = \left[\begin{array}{c|c} W_P R_{in} & -W_P G_{aug} \\ 0 & W_u \\ \hline R_{in} & -G_{aug} \end{array}\right] \begin{bmatrix} \begin{bmatrix} w_1 \\ w_2 \end{bmatrix} \\ u \end{bmatrix} \tag{1.8}$$

As stated in Question 7, we define G_{aug} as the series interconnection of G_{in}, G and G_{out} as in Equation 1.9 since the nominal system effectively means $\Delta = 0$.

$$G_{aug} = G_{out} G G_{in} \tag{1.9}$$

Question 10

The generalized plant P has 6 states. This is a combination of the states comprising the performance weights as well as the actual system dynamics represented by the system G.

G has 2 states

Wu has 3 states

Wp has 1 state

By augmenting these systems, we result in a system with a total of 6 states. Note that choosing alternative input and performance weights W_u, W_P, we could potentially have a generalized plant P with more/less states.

Question 11

N can be formulated using the sub-blocks of the P matrix in Equations 1.7 as

$$N = P_{11} + P_{12} K \big(I - P_{22} K\big)^{-1} P_{21}. \tag{1.10}$$

where the entries P_{11} through P_{22} are defined in Equation 1.8. Alternatively, the matrix N can be constructed by directly considering the z-to-w input-output relation describing the performance weights. Since we only consider a control input weight W_u and a performance weight W_P, N is defined as

$$z = Nw \quad \Longrightarrow \quad N = \begin{bmatrix} W_u K S \\ W_P S \end{bmatrix} \tag{1.11}$$

Question 12

In the nominal case, the controller should only consider the differences $e_1 = \eta_c - \eta$ and $e_2 = q_c - q$. Since we do not consider the variable z_Δ, the third element of controller K will be 0. In this case, using *hinfsyn*, we obtain the controller $K(s)$ as

$$K(s) = \begin{bmatrix} K_1(s) & K_2(s) & 0 \end{bmatrix} \tag{1.12}$$

By inspecting Figure 8 and computing the open-loop poles of the system, a Nyquist stability analysis can be performed. The open-loop system (P11) has LHP poles. Since $det(I + L(jw))$ does not encircle the origin, the first Nyquist criteria is met [2]. Furthermore, Figure 8 shows that $det(I+L(jw))$ does not pass the origin, meeting the second criteria [2]. Hence, we can conclude through the Nyquist criteria that the closed-loop system is stable.

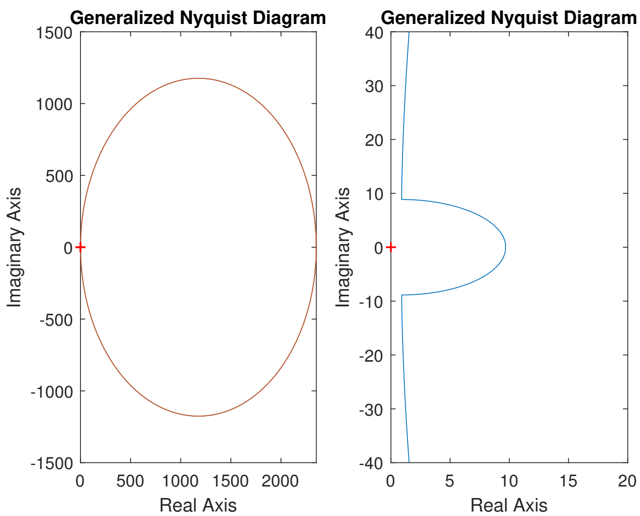

Figure 8: Generalized Nyquist diagram

Question 13

Taking the H_∞ norm on the transfer matrix N yields

$$||N||_\infty = 0.428.$$

The nominal performance requirement is that the H_∞ norm of the weighted sensitivity, $W_P S$, must be less than one. Since the transfer matrix N, containing $W_P S$, is below this bound, we have nominal performance.

Question 14

The controller has 6 states, which is the same as the amount of states of the generalized plant P as stated in Question 10. This is based on the way in which the mixed-sensitivity optimization is performed since it uses the same structure (states) as the generalized plant to converge towards a controller K.

By choosing more complex performance weights (i.e. weights with more states), the amount of states of the generalized plant P will increase, which will automatically increase the amount of states in the controller synthesized by the mixed-sensitivity optimization routine. In other words, since the amount of states of the generalized plant P and the controller are equal, by altering the amount of states in P, the amount of states in the controller K will also change.

Question 15

Figure 9 shows a step response of the input η_c for the system using the mixed-sensitivity controller. These results can be directly compared to Figure 5. Note a greater initial dip in the η value in Figure 9 as opposed to Figure 5. On the other hand, q is less oscillatory using the mixed-sensitivity controller.

Compared to the SISO controller, we notice slightly improved performance when considering the typical step response metrics. The final performance parameters for the $\eta_c - \eta$ tracking using the mixed-sensitivity controller are

- Overshoot: 0%
- Settling time: 0.76s
- Rise time: 0.43s

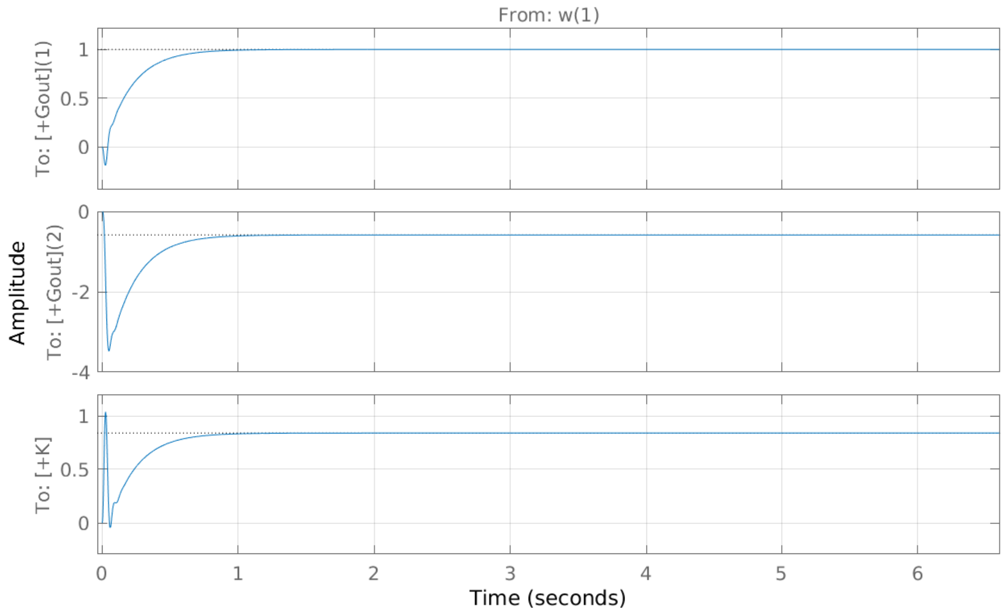

Figure 9: Step response η, q, u

Question 16

The maximum allowable control signals can be decreased by increasing the penalty function W_u. Hereby avoiding high frequency oscillations on the input. By increasing the weight W_u and possibly also decreasing the weight W_P which will allow diminish the peak of the input sensitivity function KS.

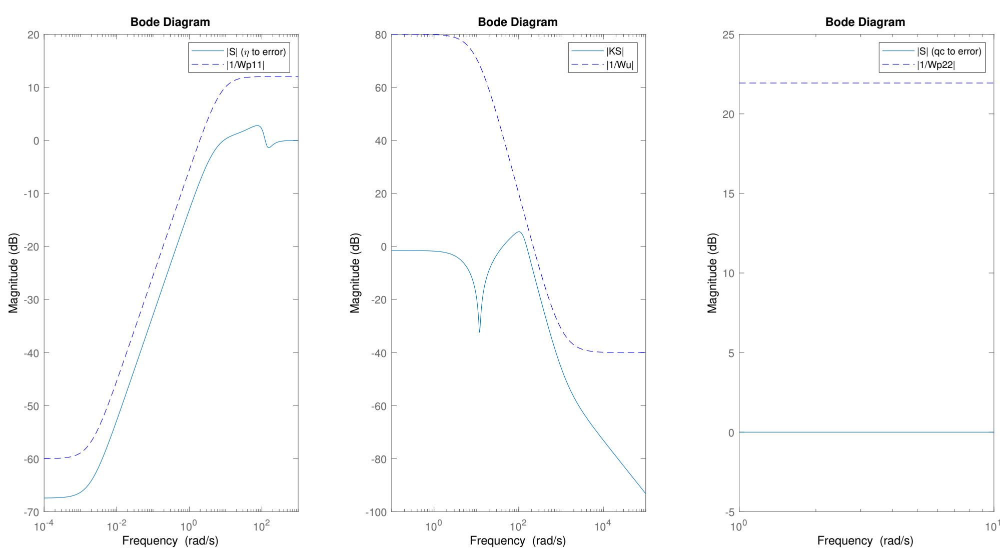

Figure 10: Sensitivity plot vs. corresponding penalty functions. As expected, all sensitivity functions lie below its corresponding penalty function since the H_∞-norm of N lies below 1 (Q13).

Question 17

From the graphs depicted in Figure 10, the $||N||_\infty$ can be roughly estimated by looking at the distance between the two lines which yield the smallest distance. This is because the H_∞ norm is essentially the maximum peak value of each graph, and the location where the two lines are closest, indicate an H_∞-norm closest to 1.

A small distance indicates an H_∞ value closer to one. Two lines who lie relatively further imply an H_∞-norm closer to zero. If the sensitivity function were to cross the penalty functions, H_∞ will be larger than one. However, this is not the case as shown in Figure 10.

Question 18

Figure 11 shows a comparison of the SISO controller and the mixed-sensitivity controller in the time-domain. It is worth noting the comparatively smooth response of the mixed-sensitivity controlled system's output. The mixed-sensitivity controller's step response also does not result in any overshoot, compared to the SISO response.

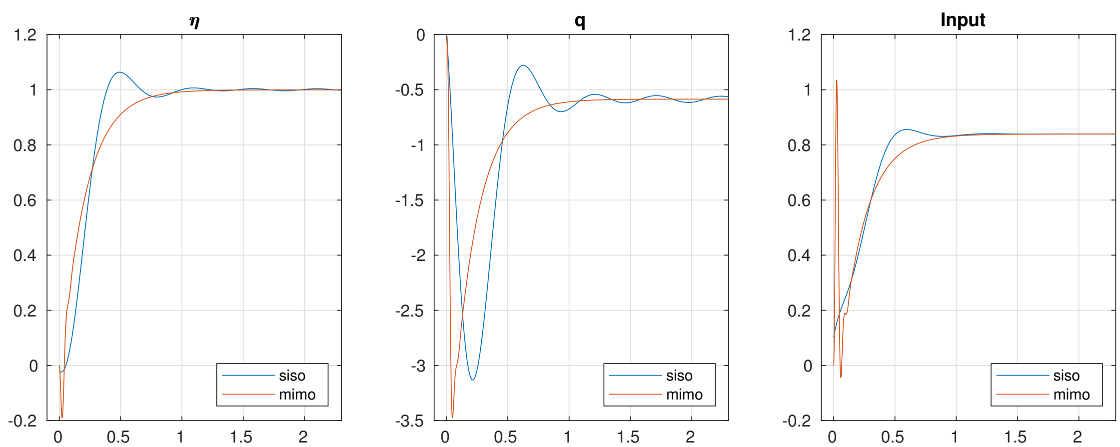

Figure 11: Comparison of SISO and Hinfsyn Controllers

Considering the frequency domain, Figures 12 and 13 show the open-loop bode plots of the η channel for the SISO and MIMO controller respectively. Figures 14 and 15 show the corresponding Nyquist plots. Despite both systems being stable (large PM and GM), we note that the MIMO controller has an increased phase margin (82^o vs 62.4^o) compared to the SISO controller. This is backed-up by the lack of overshoot of the MIMO controller response as shown in Figure 11. On the other hand, we do note a slightly higher bandwidth of the SISO controller which indicates a slightly faster response.

Two Fundamental differences between the two techniques are:

1. The H_∞ controller synthesis is an automated design which uses the infinity norm of the output function to find an optimal controller (optimal in terms of lowest maximum singular value). On the other hand, SISO loop-shaping is a manual method which requires an iterative trial-and-error based process to alter the open-loop transfer function.

2. Since inputs and outputs are interconnected, bode plots of input-to-output transfer functions only give accurate information regarding the system performance in the SISO case. The mixed-sensitivity optimization therefore uses a different metric to find the optimal controller i.e. the infinity norm of the system outputs. The SISO loop-shaping method of course uses

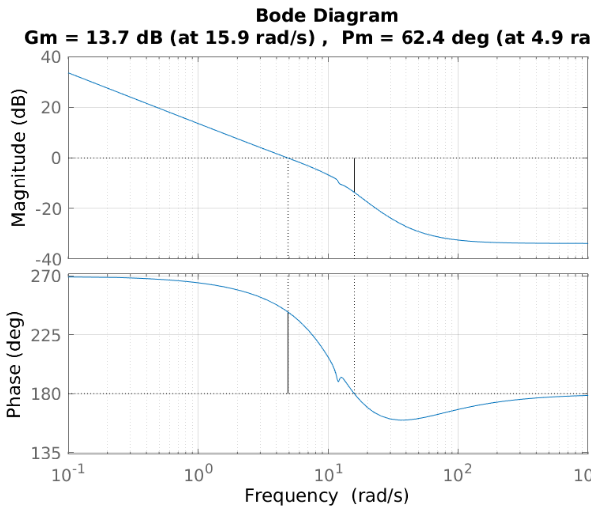

Figure 12: SISO Controller Bode Plot

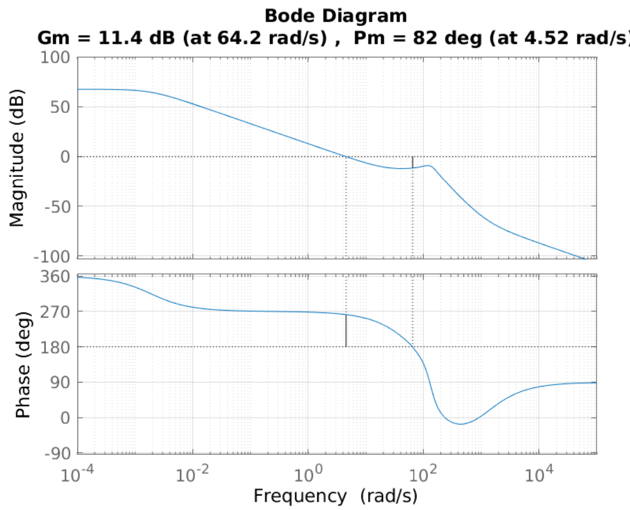

Figure 13: MIMO Controller Bode Plot

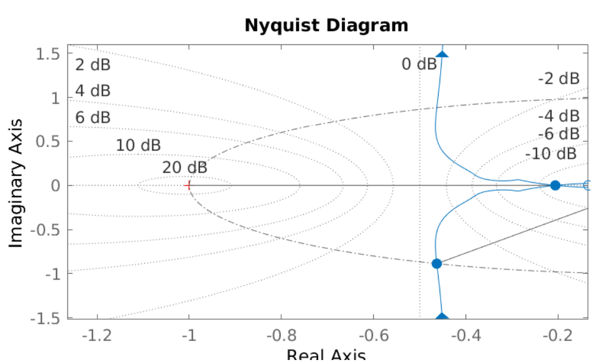

Figure 14: SISO Controller Nyquist Plot

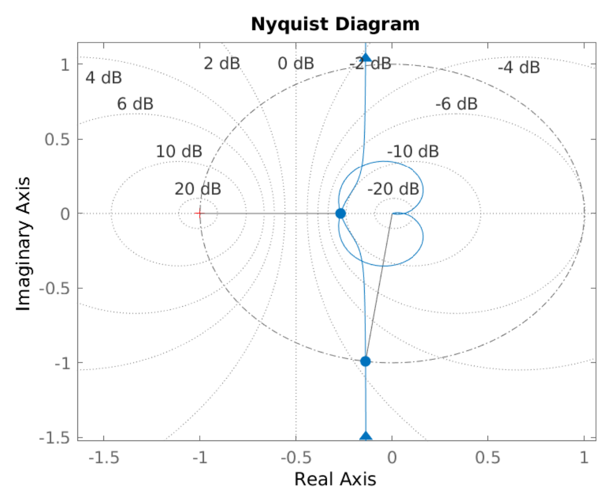

Figure 15: MIMO Controller Nyquist Plot

2 Robust Analysis and Robust Control Design

Question 19

To plot the singular values of the uncertain open-loop system, we first define the open-loop transfer function from input u to output y of the dynamical system. This relation is defined in Equation 2.1.

$$\frac{Y(s)}{U(s)} = G_{\text{out}} G \big(I - W_d \Delta Z_d G\big)^{-1} G_{\text{in}} \tag{2.1}$$

Figure 16 shows the open-loop singular values for different Δ values as defined in Equation 2.1. It is interesting to note the large variation of different possible frequency responses.

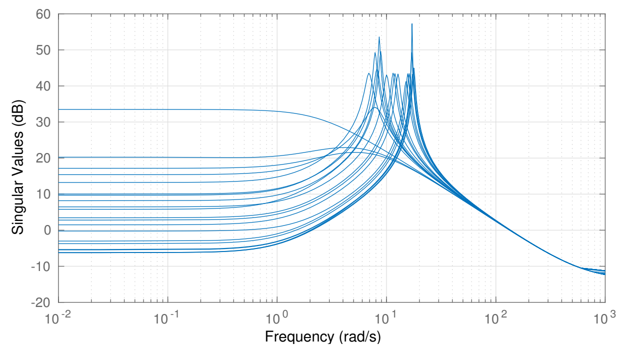

Figure 16: Singular Values of Uncertain Open-Loop System

Question 20

In order to design an uncertainty weight W_Δ, Equation 7.28 from [2] is repeated in Equation 2.2. Choosing $r_0 = 0.2$ and $r_\infty = 1.0$, with $\tau = \frac{1}{100} rad/s$, we obtain a weight $W_\Delta(s)$ as shown in Equation 2.3. Figure 17 shows the singular values of Question 19, but with the added performance weight W_Δ. Note a high emphasis around 10 rad/s and a lower emphasis at lower frequencies as defined by W_Δ in Equation 2.3.

$$w_I(s) = \frac{\tau s + r_0}{\frac{\tau}{r_\infty} s + 1} \tag{2.2}$$

$$W_\Delta(s) = \frac{0.01s + 0.2}{0.01s + 1} \tag{2.3}$$

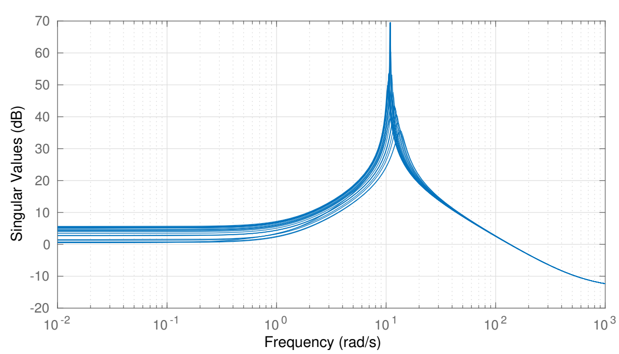

Figure 17: Singular Values of Weighted Uncertain Open-Loop System

Question 21

To obtain a generalized expression of the plant with uncertainty and external controller, we first consider the block diagram and map the inputs Δu, w, u to the outputs Δy, $z = \begin{bmatrix} z_1 & z_2 \end{bmatrix}^T$, v. Considering the block diagram, the following P matrix was obtained as in Equation 2.4. Note the exclusion of the uncertainty weighting W_Δ as defined in Equation 2.3, as well as inclusion of the pre-defined performance and input weights W_P and W_u respectively.

$$\begin{bmatrix} \Delta y \\ z \\ v \end{bmatrix} = \underbrace{\begin{bmatrix} P_{11} & P_{12} & P_{13} \\ P_{21} & P_{22} & P_{23} \\ P_{31} & P_{32} & P_{33} \end{bmatrix}}_{P} \begin{bmatrix} \Delta u \\ w \\ u \end{bmatrix}$$
$$\begin{bmatrix} \Delta y \\ \begin{bmatrix} z_1 \\ z_2 \end{bmatrix} \\ v \end{bmatrix} = \begin{bmatrix} Z_d G W_d & 0 & Z_d G G_{in} \\ -W_P G_{\text{out}} G W_d & W_P R_{\text{in}} & -W_P G_{\text{out}} G G_{\text{in}} \\ 0 & 0 & W_u \\ -G_{\text{out}} G W_d & R_{\text{in}} & -G_{\text{out}} G G_{\text{in}} \end{bmatrix} \begin{bmatrix} \Delta u \\ w \\ u \end{bmatrix} \tag{2.4}$$

Question 22

We can now define N assuming that the controller K has already been synthesized. Essentially, we define $u = Kv$ and define the mapping between the inputs Δu, w and the outputs Δy, z as shown in Equation 2.5.

$$\begin{bmatrix} \Delta y \\ z \end{bmatrix} = \underbrace{\begin{bmatrix} N_{11} & N_{12} \\ N_{21} & N_{22} \end{bmatrix}}_{N} \begin{bmatrix} \Delta u \\ w \end{bmatrix}$$

$$\begin{bmatrix} \Delta y \\ \begin{bmatrix} z_1 \\ z_2 \end{bmatrix} \end{bmatrix} = \left[\begin{array}{c|c} Z_d G\big(I + G_{in} K G_{out} G\big)^{-1} W_d & Z_d G\big(I + G_{in} K G_{out} G\big)^{-1} G_{in} K R_{in} \\ \hline -W_p\big(I + G_{\text{out}} G G_{\text{in}} K\big)^{-1} G_{\text{out}} G W_d & W_p\big(I + G_{\text{out}} G G_{\text{in}} K\big)^{-1} R_{\text{in}} \\ -W_u K\big(I + G_{\text{out}} G G_{\text{in}} K\big)^{-1} G_{\text{out}} G W_d & W_u K\big(I + G_{\text{out}} G G_{\text{in}} K\big)^{-1} R_{\text{in}} \end{array}\right] \begin{bmatrix} \Delta u \\ w \end{bmatrix} \tag{2.5}$$

We can define F as done in [2] and repeated in Equation 2.6.

$$F = F_u(N, \Delta) \triangleq N_{22} + N_{21}\Delta\big(I - N_{11}\Delta\big)^{-1} N_{12} \tag{2.6}$$

Note that to test the robust stability of F, we can consider the $M\Delta$-structure where $M = N_{11}$ since $\Delta y = M\Delta u$. This makes intuitive sense since nominal stability requires N_{11}, N_{12}, N_{21} and N_{22} to be stable, i.e. N must be internally stable. Therefore, if we can show that $M\Delta < 1 \forall \omega, \forall \Delta \in \bar{\Delta}_{\text{struct}}$, then we can state that $\det(I - M\Delta) \neq 0$ which implies that F will be stable since each sub-element of F as described in Equation 2.6 is stable.

Question 23

F can be defined as the set of perturbed transfer functions from input w to output z. From page 300 of [2]:

$$F = W_p S_p \tag{2.7}$$

Where S_p is the set of uncertain sensitivity functions and W_p is the performance weight. From the bode-magnitude plot of $1/W_p$ vs. S_p robust performance can be evaluated and if indeed $||F||_\infty \leq 1$ is achieved.

Figure 18 shows S_p does not lie below its penalty function and hence, in this case, robust stability is not achieved.

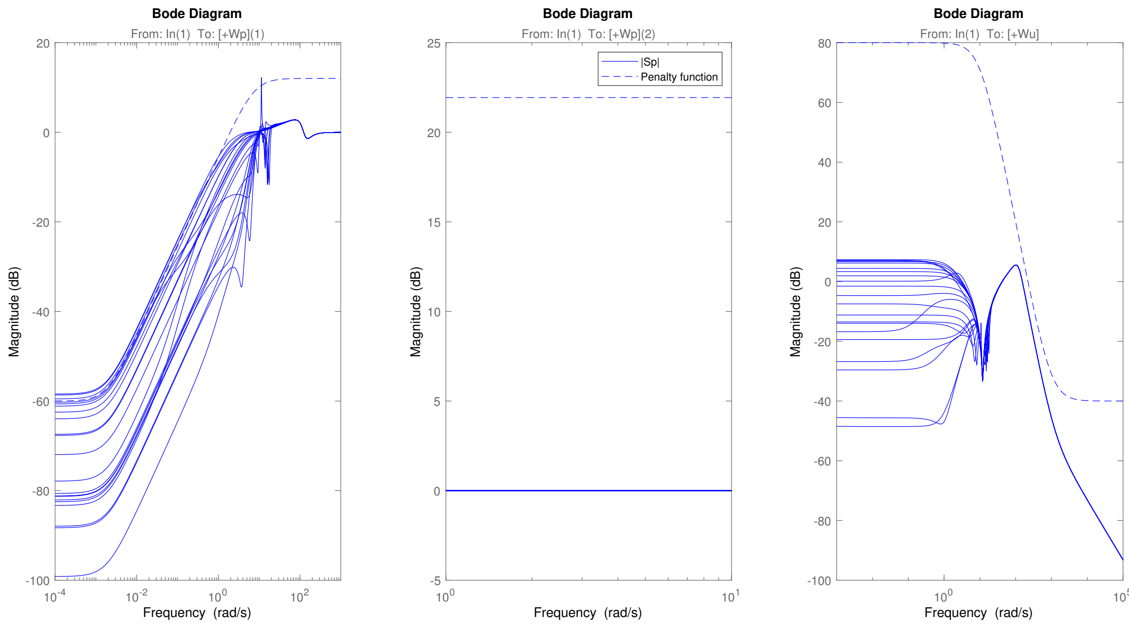

Figure 18: Evaluating robust performance using S_p and $1/W_p$.

Question 24

The problem is that since $F = F_u(N, \Delta)$ is a function of Δ, it has infinitely many possible values, since Δ itself is a variable representing a set of infinitely many values as long as $||\Delta||_\infty \leq 1$. It is therefore difficult to find the infinity norm of F analytically since it would require us to evaluate F at infinitely many values of Δ. This is illustrated in Figure 19.

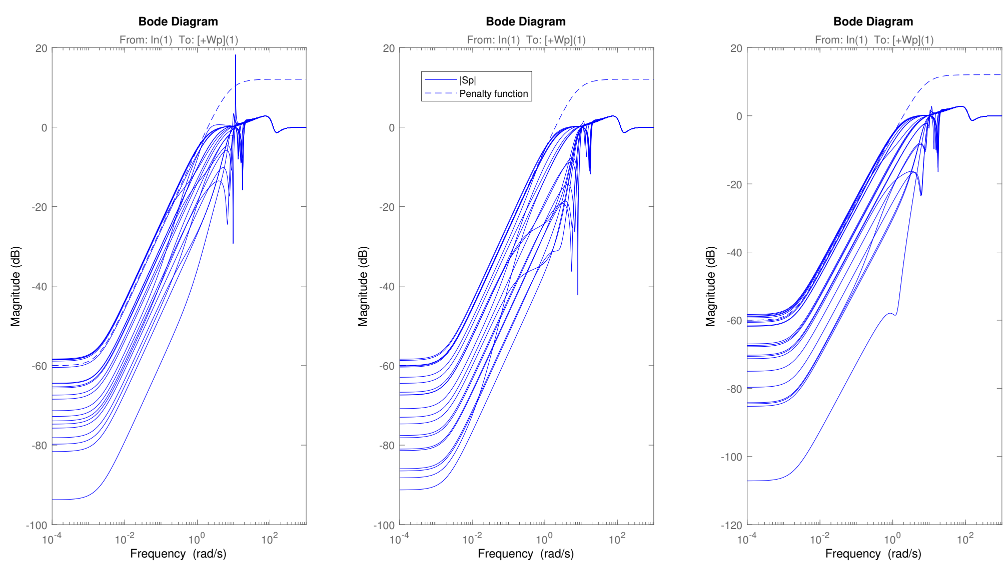

Figure 19: Due to the set of infinitely many values of F, the sensitivity is not constant. This makes it difficult to make stability assumptions based on F.

To overcome this, the structured singular value was derived which provides a bound on functions containing these uncertainties represented by Δ. This is further explored in the subsequent questions.

Question 25

Using the controller K which was designed in Question 12, we can transform the system to $M\Delta$-structure and $N\Delta$-structure to check for robust stability and robust performance respectively.

Nominal Stability

We check if N is internally stable. This is done by checking whether each sub-entry of N, namely N_{11}, N_{12}, N_{21}, N_{22} is stable. We do this by ensuring all the eigenvalues of each block is in the left half plane.

The largest real-part of all the eigenvalues of the N blocks is -0.0019, implying that the system is internally stability implying nominal stability.

Nominal Performance

For nominal performance, we require $\bar{\sigma}(N_{22}) < 1, \forall\omega$ as well as nominal stability. We have already shown that we have nominal stability.

The largest singular value of N_{22}, $\bar{\sigma}(N_{22}) = 0.4277 < 1$ which means we do have nominal performance.

Robust Stability

For robust stability, we require the structured singular value $\mu_\Delta(N_{11}) < 1, \forall\omega$. Using the definition of $M = N_{11}$, we find that $\mu_\Delta(N_{11}) = 17.7641$ meaning that the controlled system is not robustly stable.

Robust Performance

Without even applying the equations below, we already expect to not have robust performance, since we do not have robust stability. The analysis below is done simply for completeness and to tie in with Question 29 where we check for these properties again.

As detailed in Lecture 6, slide 12, robust performance can be determined by ensuring that

$$\mu_{\hat{\Delta}}(N) < 1, \quad \forall\omega, \quad \hat{\Delta} = \begin{bmatrix} \Delta & 0 \\ 0 & \Delta_P \end{bmatrix} \tag{2.8}$$

Using this scheme, we obtained $\mu_{\hat{\Delta}}(N) = 18.08 > 1$ which confirms that the system is not robustly performant.

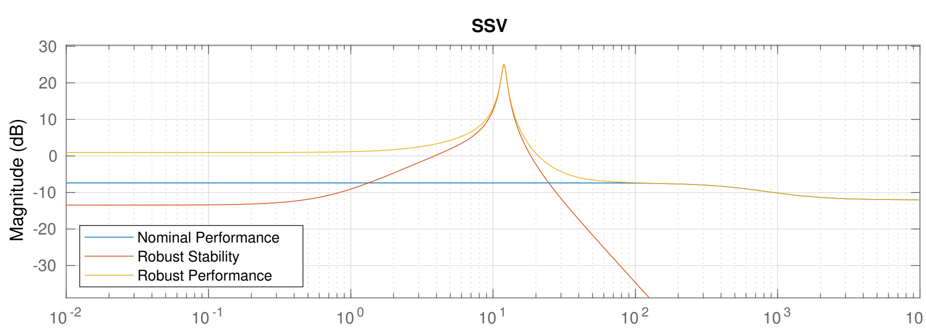

Figure 20: SSVs of NP,RS,NP for mixed sensitivity controller

Figure 20 shows the SSVs of the related NP, RS, RP analyses. Note the peak in the RS and RP graphs at around 10 rad/s which show that the controlled system is not stable around this frequency, and ultimately, not robustly stable or performant.

Question 26

We could use Nyquist to determine RS and RP. This would give a more graphical interpretation compared to SSV, which outputs a value. Robust performance through general Nyquist is guaranteed if the follow inequality holds :

$$|\omega_P S| + |\omega_I T| < 1, \forall\omega \tag{2.9}$$

Robust stability can be guaranteed through general Nyquist if the following inequality holds:

$$|1 + L(j\omega)| > |\omega_I L(j\omega)|, \forall\omega \tag{2.10}$$

Equations 2.9 and 2.10 are visualized in Figure 21.

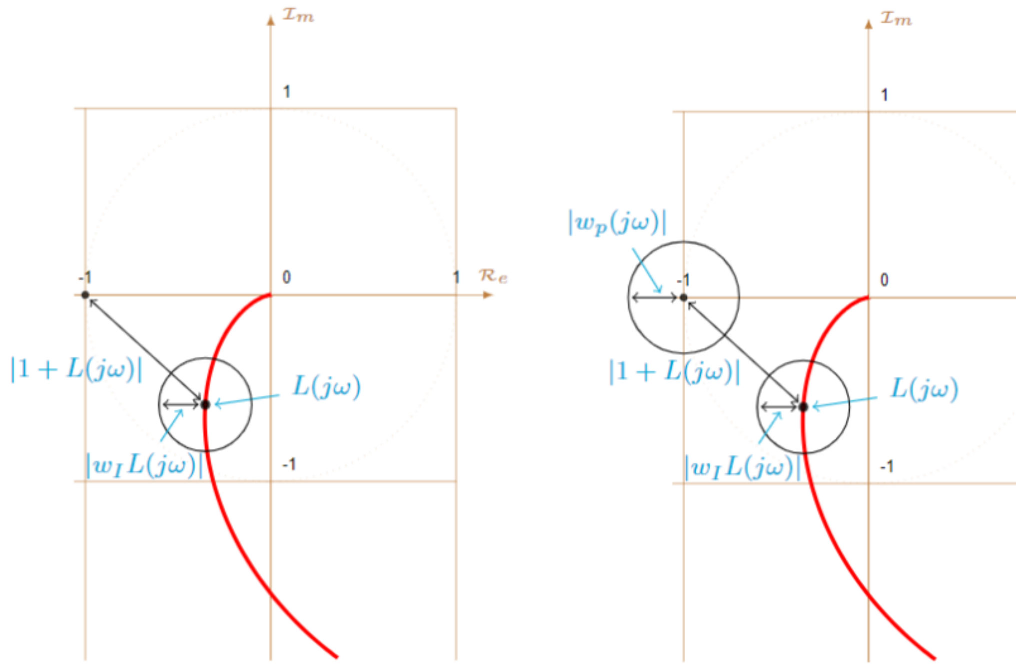

(a) Robust stability Nyquist criteria

(b) Robust performance Nyquist criteria

Figure 21: RP and RS criteria Nyquist. Source: TU Delft, [SC42010] Lecture slide L4

Question 27

As defined by the conditions stated on page 319 of [2], it can be concluded that the value of μ affects NP through the following inequality:

$$NP \leftrightarrow \bar{\sigma}(N_{22}) = \mu_{\Delta_P} < 1, \forall\omega \tag{2.11}$$

As was concluded in Question 13, we need to ensure that the value of $\mu < 1$ to ensure NP. The reason for this is that N_{22} relates the input w to the output z without considering the uncertainty. Hence, ensuring that this (weighted) relationship is norm-bounded by 1 will ensure nominal performance.

Robust Controller Synthesis using *DK* Iterations

Question 28

For the DK-iterations, the D-matrix will be different for the left side than the right side. This is because the plant G does not have the same amount of inputs as outputs. The D matrices will have the following structure

$$D_L = \text{diag}(d_{L1}, d_{L2}, d_{L3}, d_{L4}, d_{L5}, d_{L6}, d_{L7})$$
$$D_R = \text{diag}(d_{R1}, d_{R2}, d_{R3}, d_{R4})$$

However, since the uncertainty Δ has size 1×1, the only elements of D matrix that will change will be the $(1, 1)$ entries.

Note that D_L is 7×7 and D_R is 4×4. This is because the generalized plant has 6 outputs and 3 inputs, and the uncertainty Δ is 1×1, meaning the final dimensions of N will be $(6 + 1) \times (3 + 1) = 7 \times 4$.

This structure can be confirmed when inspecting the $dkinfo$ object of the *dksyn* command when implementing the DK-iteration algorithm in MATLAB.

Question 29

Using DK-iterations, we can synthesize a robust controller K to (hopefully) get robust stability and performance of the uncertain system we have defined in this assignment. This was done using the MATLAB command *dksyn*. We defined a generalized plant P which contains the uncertainty parameter Δ where $||\Delta||_\infty \leq 1$ and synthesized a robust controller using the DK-iterations methods as outlined in Section 8.12 in [2].

Having synthesized a controller, we perform the same analysis as in Question 25 to check for NS,NP,RS and RP.

Nominal Stability

The largest real-part of all the eigenvalues of the N blocks is -0.0019, implying that the system is internally stable and therefore *nominally stable*.

Nominal Performance

The largest singular value of N_{22}, $\bar{\sigma}(N_{22}) = 0.5393 < 1$ (and we have NS) which means the system has nominal performance.

Robust Stability

For robust stability, we require the structured singular value $\mu_\Delta(N_{11}) < 1, \forall\omega$. Using the definition of $M = N_{11}$, we find that $\mu_\Delta(N_{11}) = 0.2129$ (and we have NS) meaning that the controlled system is robustly stable.

Robust Performance

Robust performance can be determined by ensuring that

$$\mu_{\hat{\Delta}}(N) < 1, \ \ \forall\omega, \quad \hat{\Delta} = \begin{bmatrix} \Delta & 0 \\ 0 & \Delta_P \end{bmatrix}$$

Using this scheme, we obtained $\max \mu_{\hat{\Delta}}(N) = 0.5957 < 1$ (and we have NS) which confirms that the system has robust performance.

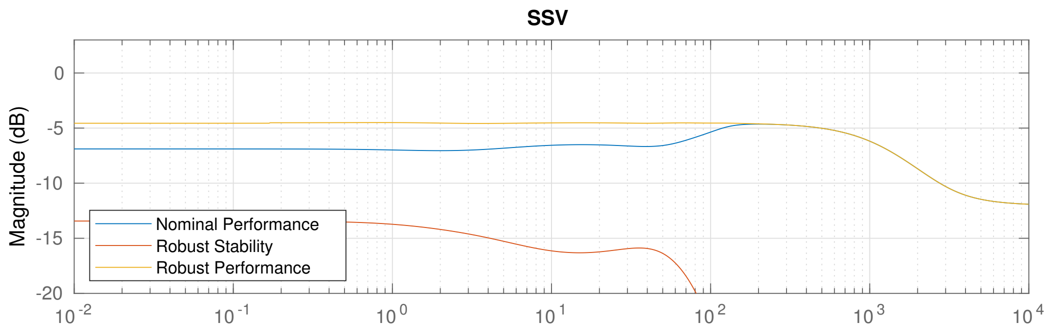

Figure 22: SSVs of NP,RS,NP for robust controller

Figure 22 shows the singular values for the NP, RS and RP analysis indicating that all the respective singular values remain below $1 = 0$dB for all frequencies.

In conclusion, the controller synthesized using DK-iterations results in a closed-loop system with up to Robust Performance. This is a vast improvement from the previous control designs where RP and even RS was not the case.

Question 30

A time-domain simulation was performed by applying a step input to each w input. Recall that w consists of reference input η_c and disturbance q. Figure 23 shows how a step input on η_c is tracked with zero steady-state error, whereas a step disturbance on q is rejected in both η and q.

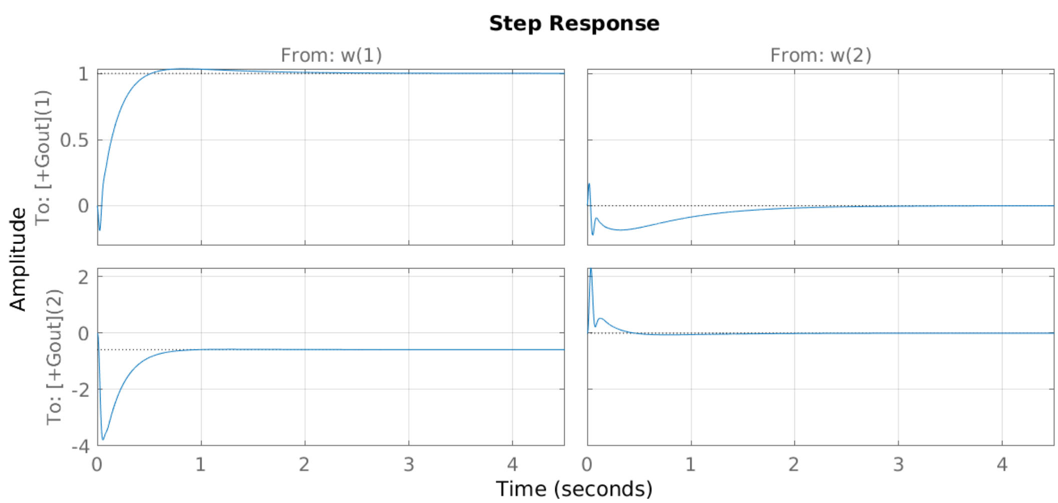

Figure 23: Step response of nominal system using robust controller

Figure 24 is a comparison in the step response on η for different Δ uncertainty constants of 0, $+1$, -1. This comparison shows a very similar response for these different uncertainties which are an indication of robust system performance. The result for NP in Question 29 is confirmed by this graph.

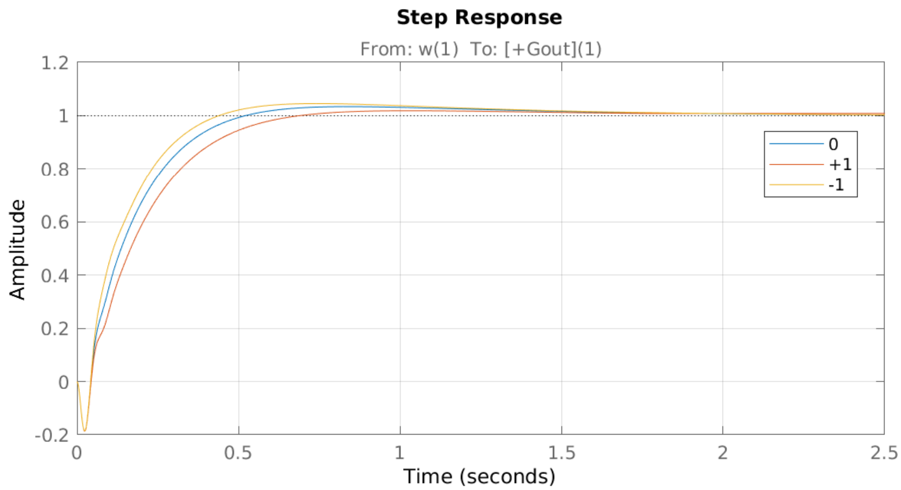

Figure 24: Step response of 0, -1, +1 disturbance using robust controller

Question 31

Here we compare the three controllers designed in Questions 4, 12 and 29. These are the SISO, mixed-sensitivity MIMO and robust MIMO controllers respectively.

To avoid repition, we reference the time-domain and frequency-domain plots for the SISO controller and MIMO mixed-sensitivity controller designs in Figures 12, 13, 14 and 15. Figures 25 and 26 show the respective bode and Nyquist plot for the open-loop system using the DK-iterations controller.

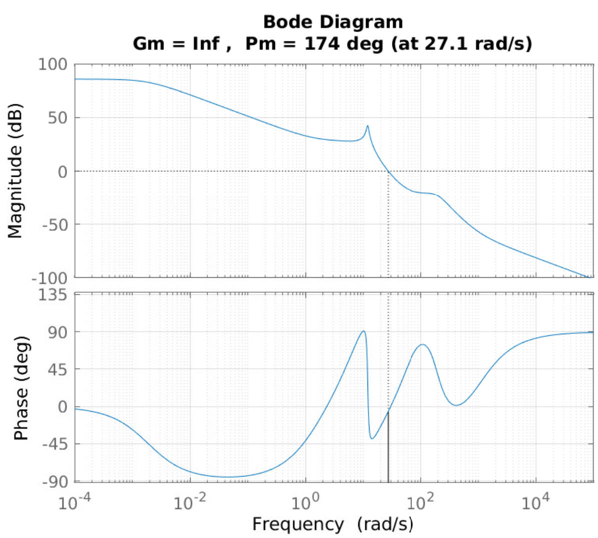

Figure 25: DKsyn Controller Bode Plot

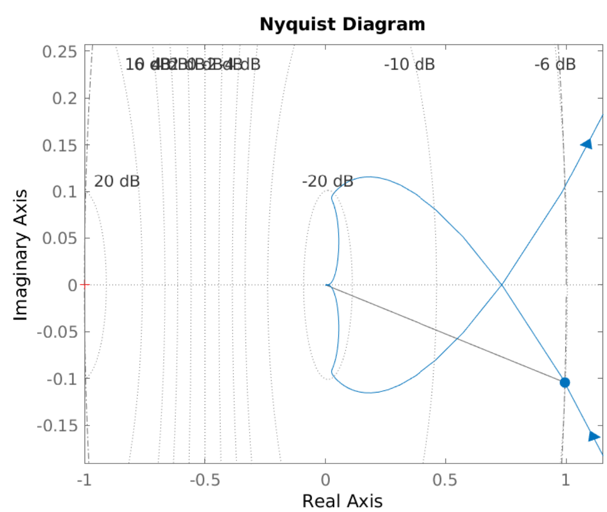

Figure 26: DKsyn Controller Nyquist Plot

Comparison and Discussion

By comparing the time-domain and frequency domain responses of the system using the three different controllers, we can conclude the following regarding the overall system performance.

SISO controller

- As shown in Figure 5, the SISO controller shows very good performance for the nominal, SISO loop (i.e. only considering the η parameter). The response is slightly more oscillatory due to a smaller phase margin 62.4^o. This compared around 80^o PM for the mixed-sensitivity and DK-iterations controllers.

- We note a step on q has an offset and is clearly not optimal, indicating a downside of SISO controllers for MIMO systems with non-identity RGA matrices.

Mixed sensitivity controller

- With the mixed-sensitivity controller, the closed-loop system does not have robust stability or performance, as mentioned in Question 25 using a SSV analysis. However, the closed-loop system does have nominal stability and performance, which would be expected, since the mixed-sensitivity controller is derived based on the nominal system.

- When only considering the η channel, the nominal system performance is better than the system using the DK-iterations controller. However, this comes at the cost of robustness, which the mixed-sensitivity controller does not have.

DK-iterations controller synthesis

- The system using this controller has robust performance and stability as shown in Question 29. This means that the Nyquist plot is stable for all possible structured inputs as described in the problem formulation in Question 28. This is not the case for the previous two controllers.

- As shown in Figure 24, applying a constant disturbance to the q channel of the system does not affect the η step response dramatically and η quickly converges to zero. This is a good indication of system robustness in the time-domain. This property was not obtained using the mixed-sensitivity and SISO controllers.

- By considering the SSV-analysis for RS and RP, we know that the system is well within the bounds (0.2129 and 0.5957) which indicates a robustly controlled system. This is also represented in Figure 22 where the SSV's are shown to be below 1 for all frequencies.

Having followed this assignment, it is interesting to note the step-by-step improvements posed by the different controller design methods:

1. SISO loop shaping is a manual tuning method where the control engineer needs to manually iterate through controller designs until a desired SISO response is obtained.

2. The mixed-sensitivity controller synthesis method can be seen as an automated loop shaping based on the $\mathcal{H}_\infty$ output minimization criteria. However, this method still requires manual re-tuning of the weighting functions to ensure robust stability and performance.

3. DK-iterations provides a possible solution which automates this iterative process using the cleverly derived structured singular value metric.

In summary, the DK-iterations controller is more desirable than the previous two. This is because this is the only controller which has robust stability and performance. This means that for all inputs w , the outputs z will be stable even if subject to the required performance weights W_u and W_P.

Optimum Comparison

Question 32

The controller described in [1] was implemented on the uncertain system and the system response to a step on η_c is shown in Figure 27

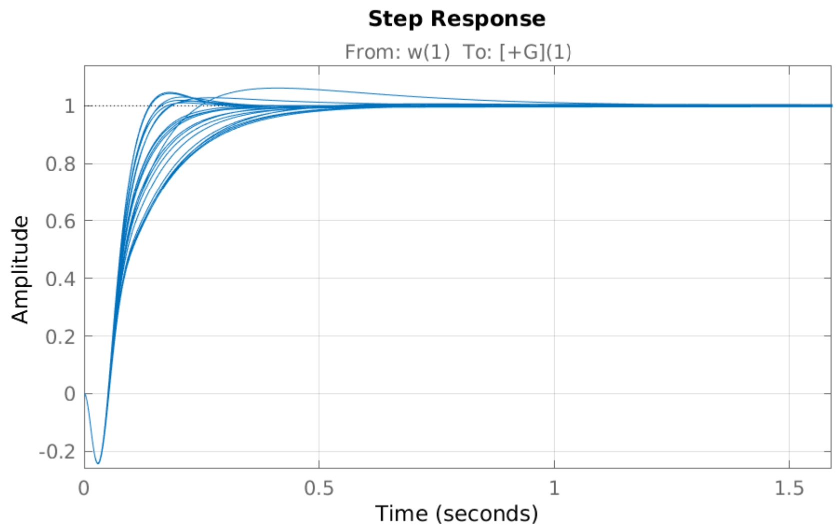

Figure 27: Step response on η

Compared to Figure 23, we note that the LMI-based controller has a faster response, albeit with more overshoot for a variety of potential uncertainty values in Δ.

Why is our time-response slower?

The paper in [1] proposes an LMI-based analysis and synthesis method for robust pole placement in LMI regions. The increased speed in the transient response of the LMI-based method is due to the fact that the controller derived in the paper only uses a performance weight W_e on the integral of the η error (as opposed to W_P), meaning that the constraints on the allowable system bandwidth are effectively diminished. This results in a controller with faster response.

Another contributing factor is that, as described in Section VI, pg. 2266, the uncertainty set described by the LMI's is slightly less conservative than that described by simply considering the H_∞ function of the uncertainties. This means that the resultant controllers are both equally robust, but the LMI-based approach is slightly faster.

MATLAB Code

References

[1] Chilali, M., Gahinet, P., and Apkarian, P. Robust pole placement in lmi regions. *Automatic Control, IEEE Transactions on 2* (01 2000), 2257 – 2270.

[2] Skogestad, S., and Postlethwaite, I. *Multivariable Feedback Control: Analysis and Design.* John Wiley & Sons, Inc., USA, 2005.